available at www.sciencedirect.com

ScienceDirect

journal homepage: www.ejconline.com

Addition of receptor tyrosine kinase inhibitor to radiation increases tumour control in an orthotopic murine model of breast cancer metastasis in bone

Pawel Zwolak[a], *Piotr Jasinski*[a], *Kaoru Terai*[a], *Nathan J. Gallus*[b], *Marna E. Ericson*[b], *Denis R. Clohisy*[c], *Arkadiusz Z. Dudek*[a,*]

[a]*Division of Hematology, Oncology and Transplantation, Department of Medicine, University of Minnesota, Mayo Mail Code 480, 420 Delaware Street SE, Minneapolis, MN 55455, USA*

[b]*Department of Dermatology,and University of Minnesota, Mayo Mail Code 480, 420 Delaware Street SE, Minneapolis, MN 55455, USA*

[c]*Department of Orthopedic Surgery, University of Minnesota, Mayo Mail Code 480, 420 Delaware Street SE, Minneapolis, MN 55455, USA*

ARTICLE INFO

Article history:
Received 9 April 2008
Received in revised form
10 June 2008
Accepted 1 July 2008
Available online 22 August 2008

Keywords:
SU11248
Radiation
Metastatic bone cancer
Bone cancer pain
Ras inhibition

ABSTRACT

The receptor tyrosine kinase inhibitor, SU11248, was added to localised radiation to evaluate the response of bone metastases and to define the basic mechanism of radiosensitisation. Treatment with SU11248 and radiation was assessed *in vitro* using cultured 4T1 breast cancer cells and *in vivo* using an orthotopic 4T1 murine mammary tumour model of breast cancer bone metastasis. Cultured 4T1 cells treated with SU11248 (1 μM) and radiation (10 Gy) showed an almost 7.5-fold increase in caspase-mediated apoptosis after 24 h of incubation, compared to either treatment alone. Mice treated with SU11248 (40 mg/kg/daily) and radiation (15 Gy/single-dose) had a relatively greater reduction in tumour growth, bone osteolysis, osteoclast maturation and microvessel density. Combined modality treatment resulted in improvements in behavioural pain assessment scores and normalisation of neurochemical changes in the spinal cord receiving primary afferent innervation from tumour-bearing femora. Our study demonstrates that SU11248 enhances the radiation control of metastatic breast tumours in bone and tumour-induced pain.

1. Introduction

Breast cancer is the second leading cause of cancer-related death in women, with metastasis representing a serious cause of morbidity and mortality. Bone is the most common site of metastatic breast cancer.[1] Despite recent advances in treating metastatic disease, the average survival time for patients with diagnosed bone relapse is 18–30 months.[2] Breast cancer bone metastases can cause osteolytic lesions, bone fractures, spinal cord compression, hypercalcaemia and significant pain in the area of the affected bone.[3] Patients with metastatic disease describe their pain as moderate in 40–50% of the cases and severe in 25–30% of the cases.[4] In addition to breast cancer, other types of primary cancers such as prostate and lung can metastasise to bone, producing osteolytic lesions.[5] The only available treatments for cancer-induced bone pain are radiation, non-steroidal anti-inflammatory drugs (NSAIDs) or opioids.[6–8] Patients with metastatic disease in bone require increasing doses of analgesic drugs to maintain adequate pain relief due to the development of analgesics tolerance.[9] In addition to the problem of tolerance, preclinical studies have unexpectedly demonstrated that opioids can paradoxically enhance cancer-induced pain[10] and stimulate growth of tumour.[11]

* *Corresponding author:* Tel.: +1 612 624 0123; fax: +1 612 625 6919.
E-mail address: dudek002@umn.edu (A.Z. Dudek).

0959-8049/$ - see front matter
doi:10.1016/j.ejca.2008.07.011

Localised radiation therapy is the standard therapy for pain control in patients with bone metastases. Pain relief can be achieved after single or multiple low- or high-dose fractions[12,13] Patients with bone metastases treated with higher total doses of radiation may have a longer duration of pain relief, compared to those treated with lower total doses. Despite improved pain control, higher radiation doses are associated with an 18% increased risk of pathologic fractures in long bones.[14] Therefore, any strategy that would improve the activity of single-dose or short-course radiation treatment would offer patients with painful bone metastases a safe alternative to multi-course radiation treatment.

SU11248 is an orally administered small-molecule inhibitor of receptor tyrosine kinase (RTK) that is selective for several RTKs on endothelial cells, pericytes and stromal cells, including platelet-derived growth factor receptor (PDGFR), vascular endothelial growth factor receptor (VEGFR), KIT and FMS-like tyrosine kinase 3 (FLT3).[15,16] In addition, SU11248 can have direct anti-tumour effects if RTK receptors are expressed on tumour cells.[17] Similar to tissue-type plasminogen activator 2, SU11248 may also make endothelial and tumour cells sensitive to radiation-induced cell death by either blocking VEGFR-2 and PDGFR on endothelial and tumour cells or disrupting the recruitment of endothelial cell precursors from the bone marrow.[18] Paradoxically, this effect may be due to angiogenic inhibition. It is well known that adequate tissue oxygenation is needed for irradiation to be effective. Vascular endothelial growth factor-blocking antibody has been reported to improve tumour blood flow, reduce tumour hypoxia and subsequently increase the biological effect of radiation.[19,20] SU11248 is expected to have a similar effect. Also, previous reports demonstrate that combination treatment with radiation and SU11248 or SU6668 can enhance tumour control.[21,22]

In this study, we demonstrate the potential usefulness of treating bone tumour growth, bone osteolysis and cancer-induced pain with combined radiation and antiangiogenic therapy using SU11248 in an orthotopic 4T1 murine mammary tumour model of breast cancer bone metastasis.[23–25]

2. Materials and methods

2.1. Cell culture

4T1 murine breast cancer cells (derived from bone metastases) were obtained from the laboratory of Dr. Denis R. Clohisy in the Department of Orthopedics Surgery at the University of Minnesota. Cells were grown in Dulbecco's modified Eagle medium (DMEM) with 10% foetal bovine serum (FBS) in a 95% humidified incubator at 37.5 °C with 5% CO_2. Cells at passages 20–25 were used for experiments. We selected this tumour model of bone metastasis using 4T1 cells orthotopically implanted in bone in order to assess uniformly the effect of therapy on pain behaviour.[23,24,26]

2.2. Animals

Experiments were performed on 6-week-old female C3H/Scid mice (Jackson Laboratories, Bar Harbor, ME) weighing 20–22 g. A murine strain was selected based on our previous experience with behavioural pain assessment in a model of bone cancer.[23,24] Mice were housed under pathogen-free conditions with a 12-h alternating light-and-dark cycle and fed autoclaved food and water ad libitum. All procedures were approved by the Animal Care and Use Committee at the University of Minnesota.

2.3. Cell proliferation assay

Cell Counting Kit-8 assay (CCK-8, Dojindo Corp., Japan) was used to measure cellular proliferation/cytotoxicity. Cell lines were seeded into a 96-well plate (3×10^3 cells/well). Cells were cultured in a 10% FBS medium containing 100 μl DMEM overnight to allow for cell attachment. Cells were incubated in serum-starved medium for 24 h and then treated with SU11248 at concentrations of 0.01, 0.1 and 1 μmol/l dissolved in dimethylsulfoxide (DMSO) and/or gamma irradiation at 10 Gy. Cells were then assayed using a CCK-8 assay kit. A Model 68 Cesium-137 gamma irradiator was used for *in vitro* experiments (J.L. Shepherd and Associates, Glenwood, CA). DMSO in concentration of 0.1% was used as a vehicle control. Absorbance was measured at 450 nm using an ELISA microplate reader to quantify the number of viable cells. All assays were performed in five wells and repeated at least three times with similar results.

2.4. Apoptosis/caspase detection assay

Activated poly-caspases (caspase-1, -3, -4, -5, -6, -7, -8 and -9) in living 4T1 cells were detected using the carboxyfluorescein-labelled fluoromethyl ketone (FMK)-peptide-inhibiting substrate of caspases (Immunochemistry Technologies, LLC, Bloomington, MN). Apoptosis was monitored using the Poly-Caspases (FLICA) activity kit, which contains a green fluorescent-labelled inhibitor of caspase activity, FAM-VAD-FMK, which is a cell permeable molecule consisting of a carboxyfluorescein (FAM) derivate of valylalanylaspartic acid (VAD) fluoromethyl ketone (FMK). In brief, a 6-well plate was seeded with 4T1 cells (1×10^6) in 2 ml of medium per well. Cells were treated with SU11248 (1 μmol) and/or irradiation (10 Gy) for 4, 12, 24, 48 or 72 h. The medium was removed, and the FAM-VAD-FMK FLICA reagent was added at the concentration stipulated in the manufacturer's instructions. Fluorescent-labelled apoptotic cells were counted using a flow cytometer (FACScalibur, BD Biosciences, San Jose, CA).

2.5. Caspase-3 and -9 measurements

Caspase-3 and -9 activity was analysed using the Caspase-Glo® luminescent-based assay (Promega, Madison, WI) according to the manufacturer's instructions. Cells (3×10^3) were seeded in the 96-well white opaque plates and a corresponding optically clear 96-well plate. Cells were allowed to adhere overnight and then were treated with varying concentrations of SU11248 for 12 and 24 h. The appropriate Caspase-Glo reagent (100 μl) was added to wells containing either 100 μl of blank negative control or treated cells in culture medium. Plates were gently mixed and incubated for 1 h at room temperature. Luminescence was read in a luminometer. The corresponding 96-well clear plate was used to measure

the number of viable cells with the CCK-8 reagent. Caspase activity was normalised to these values.

2.6. Immunoprecipitation assays and immunoblotting analysis

4T1 cells were seeded in tissue culture dishes (100 × 20 mm) in 10% FBS medium and incubated with SU11248 (1 μM) for 0, 2, 4, 8, 12 and 24 h. Cells were next resuspended in 1 ml of lysis buffer for 2 min, scraped and immediately snap frozen in liquid nitrogen. For Ras, lysates were resuspended in Mg^{2+}/wash buffer (25 mM HEPES at pH 7.5, 150 mM NaCl, 1% Igepal CA-630, 10 mM $MgCl_2$, 1 mM EDTA and 2% glycerol). For AKT and ERK1/2, lysates were resuspended in cell lysis buffer (20 mM Tris–HCl at pH 7.5, 150 mM NaCl, 1 mM Na_2EDTA, 1 mM EGTA, 1% Triton, 2.5 mM sodium pyrophosphate, 1 mM beta-glycerophosphate, 1 mM Na_3VO_4 and 1 μg/ml leupeptin). Protein concentration was determined with the BioRad protein assay (BioRad Laboratories, Hercules, CA). Ras affinity precipitation was performed with Raf-1 RBD agarose beads according to the manufacturer's instructions (RAS activation assay kit; Upstate, Temecula, CA). Cell lysates were subjected to SDS–PAGE followed by electroblotting onto nitrocellulose membranes. The membranes were incubated overnight at 4 °C with one of the following primary antibodies: phospho-Akt, Akt, phospho-ERK1/2 and Erk1/2 (Cell Signalling, Boston, MA), and actin (Santa Cruz Biotechnology, Santa Cruz, CA). Immunoreactive proteins were detected by incubating blots with alkaline phosphatase-conjugated secondary antibody for 1 h followed by ECF fluorescent substrate for 5–7 min. The Storm™ fluorescent scanning system (GE Healthcare, Piscataway, NJ) was used to visualise immunoreactive proteins.

2.7. Tumour model

Cultured 4T1 cells (90% confluence) were harvested after a 3-min exposure to 0.25% trypsin. Trypsinisation was stopped with a medium containing 10% FBS, and cells were washed once with a medium containing 10% FBS and then resuspended in Hank's Balanced Salt Solution (HBSS; Sigma, Deerfield, IL). Only suspensions consisting of single cells with >90% viability were used. The 4T1 injection technique was performed as described previously.[24,27] Briefly, a general anaesthetic cocktail of ketamine (97.5 mg/kg) and xylazine (37.5 mg/kg) was administered intraperitoneally. A 28-gauge boring needle was inserted, via arthrotomy, into the medullary canal to create an indentation for the cells. Ten sham-treated animals were injected with HBSS into the intramedullary space of the left femur, whereas 40 animals were injected with 4T1 cells (1×10^4). A small amount of bone wax was used to seal the injection site, thereby confining the tumour cells or HBSS within the medullary space.

2.8. Treatment groups

Treatments were administered 7 d after the intrafemoral injection of 4T1 cells into C3H/scid mice. All animals injected with 4T1 developed lytic lesions documented radiologically, and were randomised into one of the four groups consisting of ten mice per group: (A) daily oral administration by gavage of SU11248 at 40 mg/kg dissolved in 5% DMSO/saline solution, (B) single-dose of local orthovoltage irradiation of the femur at 15 Gy in one fraction, as previously described,[23,27] (C) the combination of treatments described in A and B and (D) a tumour-bearing control group receiving daily oral administration of DMSO solution in an equivalent volume as animals in group A, and who were restrained for an equivalent time as animals in group B. A non-tumour-bearing, saline-injected control group receiving daily oral administration of DMSO solution in equivalent volume was also included as a control group. The treatment regimen with SU11248 was adapted based on the previously reported results on efficacy of this compound.[28]

As previously described by Goblirsch et al.,[27] a 15 Gy dose of orthovoltage radiation was delivered to the left femur of anesthetised mice lying on a modified Broome Style Restrainer (551-BSRR, Plas-labs, Inc., Lansing, MI) using a Philips RT250 orthovoltage unit (Philips Medical Systems, Hamburg, Germany). Mice were irradiated one at a time to ensure the delivery of a dose of 15 Gy to the surface of the femur. The total dose delivered to the bone was approximately 30 Gy due to the increased absorption of X-rays in bone.[27]

2.9. Radiographic evaluation of bone destruction

Femur radiographs were taken on days 7, 13 and 16 after tumour cell and sham injections, using an X-ray machine (Faxitron X-ray Corp., Wheeling, IL). Images were captured on Kodak Min-R 2000 mammography film (Eastman Kodak Co., Rochester, NY; exposure settings: 7 s, 21 kVp). The assessment of bone destruction was performed on days 13 and 16 by a single investigator blinded to group assignments. A grading system of bone lysis with numeric values ranging from 0 to 4 was used as described previously.[24,29] The bones were harvested on day 16 (9 d after treatment). Haematoxylin and eosin (H&E) staining was used to confirm the presence of tumour in bone radiographs.

2.10. Osteoclast quantification

Bones were decalcified by 10-day exposure to phosphate buffer solution (PBS) containing 10% ethylenediaminetetraacetic acid (EDTA), and embedded in paraffin. TRAP staining of the femoral sections was used to quantify the number of osteoclasts as previously described.[30] The number of osteoclasts was calculated per square millimeter. Osteoclasts demonstrating more than three nuclei were used as a measure of osteoclast maturation.[31]

2.11. Quantification of viable tumour area and tumour necrosis in bone

All bones with tumours were fixed in formalin, decalcified and embedded in paraffin. Femoral sections, 7 μm thick, were stained with H&E to visualise the normal marrow elements and breast cancer cells under bright field microscopy. The total area of intramedullary space (bone marrow cavity) and the percent of intramedullary space occupied by tumour were calculated using Image Pro Plus v3.0 software.[24] Tumour necrosis was measured as the percent of total tumour cells showing the signs of cell death (eosinophilic cells that did

not display prominent nuclei). Viable tumour area was expressed as a percent of intramedullary space occupied by tumour cells displaying nuclei.

2.12. Quantification of microvessel density (MVD)

Bones were fixed using periodate-lysine-paraformaldehyde, decalcified and embedded in optimal cutting temperature (OCT) compound (Miles Inc., Elkhart, IN). Tissue sections (4–6 μm) were mounted on positively charged Superfrost slides (Fisher Scientific Co., Houston, TX) and dried overnight. Sections were deparaffinised in xylene, treated with a graded series of alcohol (100%, 95%, 80% ethanol/double distilled H_2O (v/v)) and then rehydrated in PBS (pH 7.5). Frozen tissues used for the identification of platelet endothelial cell adhesion molecule-1 (CD31/PECAM-1) were sectioned (8–10 μm), mounted on the positively charged Plus slides (Fisher Scientific Co., Houston, TX) and air-dried for 30 min, after which immunohistochemical studies were performed. Tumour blood microvessels were counted in sections after staining with antibodies specific to CD31 according to the methods described previously.[32] MVD was assessed by counting microvessels in five random 0.0321-mm^2 fields taken of each section at 200× magnifications.

2.13. Behavioural pain assessment

Baseline behaviours were recorded for all mice prior to tumour cell and sham injections. Behavioural assessments were next recorded on day 7 after tumour cell and sham injections but prior to the administration of control and experimental treatments. Subsequent assessments were recorded on days 13 and 16. Mice were allowed to habituate on the observation platform for 30 min before the testing commenced. Spontaneous and movement-evoked measurements of pain were recorded for each mouse. Behavioural testing included four metrics: limb use in an open field, guarding during forced ambulation, number of flinches and duration of spontaneous guarding. Limb use scores were based on a 0–4 scoring system.[24,30] Guarding scores during forced ambulation were determined using the Economex Rotarod (Columbus Instruments, Columbus, OH) set to run at a constant speed of 6 rpm. Guarding scores were defined as the time for which the animal held the affected limb completely aloft. Times for spontaneous guarding were obtained using a stopwatch to record the duration of guarding behaviour during a 2-min observation period.

2.14. Immunohistochemical preparation of spinal cords

Mouse spinal cords were immersed in Zamboni's fixative (0.03% (w/v) picric acid and 2% (w/v) paraformaldehyde) for 48 h at 4 °C and transferred to a 20% sucrose solution with 0.05% sodium azide in PBS for storage. Vertebrae were excised to expose the spinal cord, and 1 cm sections of L4/L5 were removed. Processing and staining of the cord sections were carried out according to a previously published procedure.[33] Sections were incubated in (a) polyclonal Prodynorphin (1:100) (Neuromics, Edina, MN, USA) made in guinea pig and anti-guinea pig IgG conjugated to cyanine 2 (Cy2) (1:2000) (Jackson ImmunoResearch, West Grove, PA) and (b) polyclonal glial fibrillary acidic protein (GFAP) (1:1000) made in chicken (Abcam, Cambridge, MA, USA) and anti-chicken IgG conjugated to Cy5 (1:2000) (Jackson ImmunoResearch, West Grove, PA). Samples were mounted on slide covers in agar, dehydrated in ethanol, cleared with methyl salicylate and mounted in DEPEX (Electron Microscopy Science, Poole, UK).

2.15. Image capture and integrated density quantification of immunoreactive nerves

Dorsal horn epifluorescent images of the L4–L5 spinal cord slices were acquired using a 4× lens (Olympus UPlanAPO 4X/0,16) on an Olympus Fluoview500 system (Olympus, Center Valley, PA), and their integrated densities were subsequently analysed using ImageJ. The integrated density was deemed the most biologically appropriate measurement because it takes into account the area of interest, containing dorsal horn innervation and the intensity of the epifluorescence. This technique, with slight modifications, was used for the quantification of nerves in several previous studies.[23,34–36] This volumetric approach conveys information about the depth of innervation whereas simple average grey level measurements do not. Biological variation in relation to any differences in stain absorption of individual spinal cords was accounted for by setting the grey level lower threshold at a level approximately equal to the maximum count of a sample lacking primary antibodies in order to obtain counts above the cord's observed background grey level. Total area counts of the entire cord hemisphere were also taken and factored into quantification in order to minimise the impact of the samples' biological size variability and give proper weight to each measurement. Initial counts of integrated density were divided by the cord's total area to account for the spinal cord size variation. Integrated density counts in each group were analysed using a one-way ANOVA test with Fisher's protected least significant difference (PLSD) *post hoc* test using $P < 0.05$. Images were obtained from 120-μm thick sections and captured with a Fluoview 500 confocal microscope mounted on an upright BX61 Olympus with a 10x Olympus lens and 1.5× zoom. Composite images represent 20 μm tissue and were taken in 2 μm intervals.

2.16. Statistical data analysis

Statistical significance was determined using one-way ANOVA or Student's *t*-test, as appropriate. Differences between groups in pain behaviour experiments and assessments of bone destructions scores were calculated using a proportional odds model. The generalised estimating equations (GEE) method was used to estimate parameters. A *P*-value of <0.05 was considered statistically significant.

3. Results

3.1. 4T1 Breast cancer cell death and caspase-mediated apoptosis

The effect of SU11248 on the viability of 4T1 breast cancer cells was examined after incubation in a medium containing

SU11248 at the concentrations of 0.01, 0.1 and 1 μM for 24 h. Cells incubated in the medium without SU11248 served as controls. The presence of SU11248 significantly reduced cell viability in a dose-dependent manner. This effect on cell viability was enhanced by the addition of radiation to SU11248 at a dose of $\geqslant$0.1 μM ($P < 0.05$ versus SU011248 alone) (Fig. 1A). We next examined whether SU11248 induced caspase-dependent apoptosis in the presence or the absence of radiation. 4T1 cells were treated with 1 μM of SU11248 with or without 10 Gy of radiation and incubated for 4, 12, 24, 48 or 72 h. Cells were treated with the caspase inhibitor FAM-VAD-FMK for 1 h following the radiation and/or the administration of SU11248. Caspase activity was not significantly different in 4T1 cells treated with radiation or SU11248 alone after a 24 h-period of incubation, whereas combination treatment led to an increase in the caspase-mediated apoptosis (Fig. 1B and C). To confirm this proapototic effect, we measured the activity of caspase-3 and -9 in 4T1 breast cancer cells incubated for

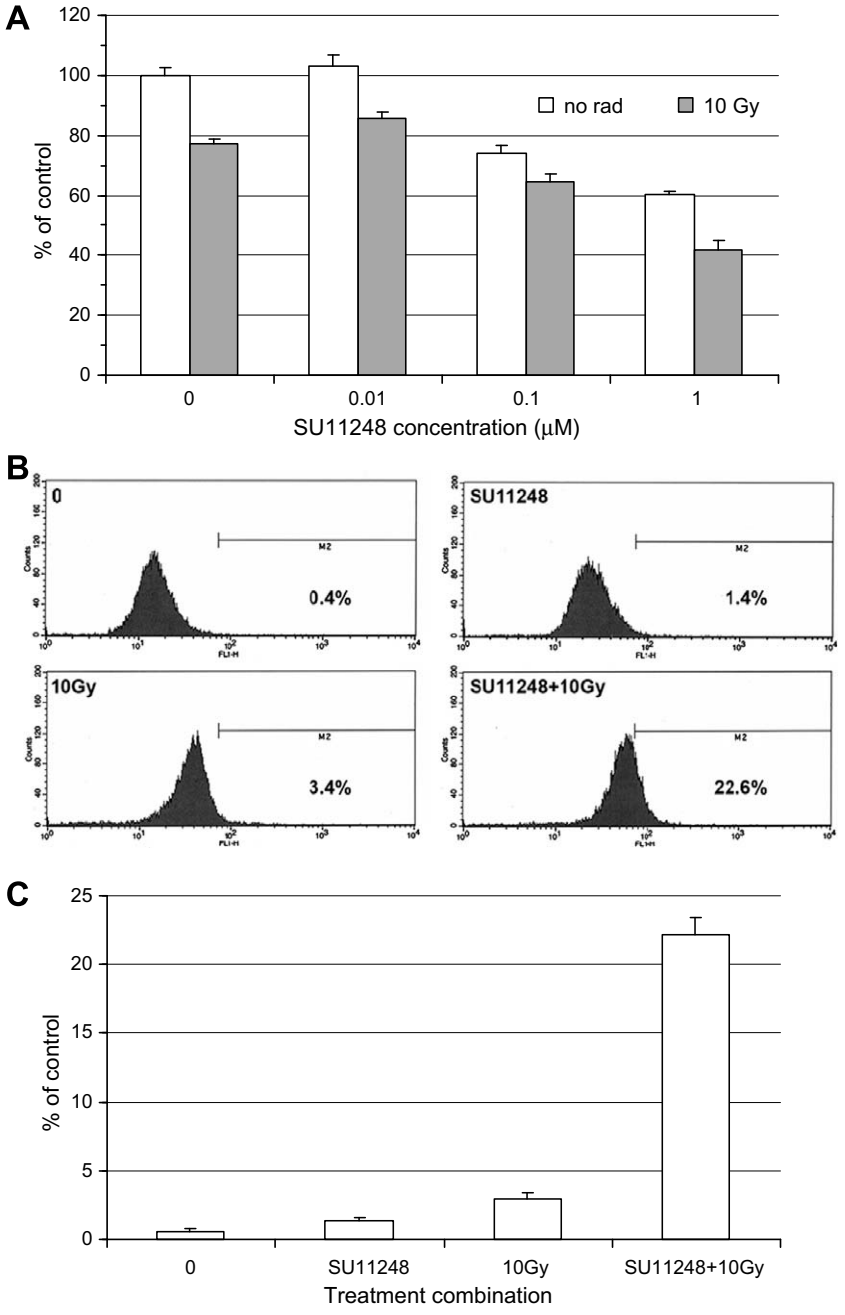

Fig. 1 – Effect of SU11248 and radiation on 4T1 cell viability and apoptosis. (A) 4T1 cell viability after 24 h of incubation with SU11248. Values represent means ± SE ($n = 3$, $^{*}P < 0.05$ versus control). (B) Synergistic effect of SU11248 and gamma irradiation on poly-caspase activation. Representative flow cytograms: Y-axis, count of events; X-axis, fluorescein intensity; caspase-positive cells lay within region M2. (C) Percentage of apoptotic cells. The means of three experiments ± SE are shown ($P < 0.001$ combination therapy versus untreated control).

12 h and 24 h with SU11248 at 0.01, 0.1 and 1 μM and/or 10 Gy of radiation. Cells incubated with SU11248 and irradiated had a statistically significant increase in caspase-3 and -9 activity in a dose- and time-dependent manner, as compared to the control cells ($P < 0.001$) (Fig. 2A and D). These results indicate that SU11248 has a radiopotentiating effect on 4T1 breast cancer cell death via a caspase-dependent activation of apoptosis. SU11248 inhibited Ras, Erk1/2 and Akt activity beginning at 4 h (Fig. 3A–C), indicating that SU11248 may enhance apoptosis by suppressing cell signalling within the Ras molecular pathway.

3.2. *Bone destruction*

Intrafemoral injections with NaCl solution had no significant impact on bone destruction except that related to needle insertion. Intrafemoral injection with 4T1 breast cancer tumour cells resulted in tumour growth with accompanying bone osteolysis and local spread to surrounding soft tissue by day 16 (Fig. 4IA and II). Nine days after treatment (day 16) with combination of SU11248 and local radiation, tumour-bearing mice had significantly less bone destruction, compared to the degree bone osteolysis seen in untreated, tumour-bearing controls (Fig. 4ID and II). Although mice treated with only radiation (Fig. 4IB) or SU11248 (Fig. 4IC) had less cortical destruction and tumour extension into the surrounding soft tissue compared to untreated, tumour-bearing controls (Fig. 4IA), this difference was not statistically significant (Fig. 4II).

3.3. *Mature osteoclasts*

Tumour-bearing mice had an increased number of osteoclasts on the tumour–bone border on day 16 (61.3 ± 21.6 osteoclasts/mm^2) compared to NaCl-injected control animals (27.5 ± 18.2 osteoclasts/mm^2). Osteoclasts were not reduced in number by treatment with SU11248, local irradiation or their combination (52.7 ± 16.9, 65.9 ± 24.8 and 58.4 ± 22.6 osteoclasts/mm^2, respectively). However, the percentage of active osteoclasts (exhibiting greater than three nuclei), which is responsible for bone lysis,[31] did significantly increase in tumour-injected mice (79.4 ± 8.6%) as compared to saline-injected mice (24.8 ± 5.2%) ($P < 0.05$ versus tumour-injected controls).

Treatment with SU11248 alone and in combination with local irradiation decreased the percentage of active osteoclasts to 45.6 ± 5.8% and 53.3 ± 3.8%, respectively, compared to the untreated, tumour-injected mice 79.4 ± 8.6% ($P < 0.05$ both treatments versus tumour-injected controls). Local irradiation did not significantly influence the number of active osteoclasts (74.8 ± 9.6%) as compared to the untreated, tumour-bearing animals, suggesting that SU11248 may have an effect on osteoclast maturation.

3.4. *Tumour burden*

Single modality treatment with SU11248 or local irradiation reduced tumour area—defined as the percent of the intramedullary space occupied by viable 4T1 cells—to 41.71 ± 6.74% and 47.49 ± 8.15% of the intramedullary space ($P < 0.05$), respectively, compared to the untreated controls. Combination treatment reduced the viable tumour area to 33.29 ± 6.04% ($P < 0.05$ versus untreated controls), suggesting that SU11248 had a radiosensitising effect on 4T1 tumour cells (Fig. 5A). Similar results were seen in the analysis of tumour necrosis area. Tumour-bearing controls showed only minimal necrosis within the intramedullary cavity, whereas animals receiving combination treatment had a significantly higher level of tumour necrosis (26.18 ± 3.84%) compared to either radiation-only (6.40 ± 3.40) or SU11248-only (14.06 ± 4.0) treatment (Fig. 5A).

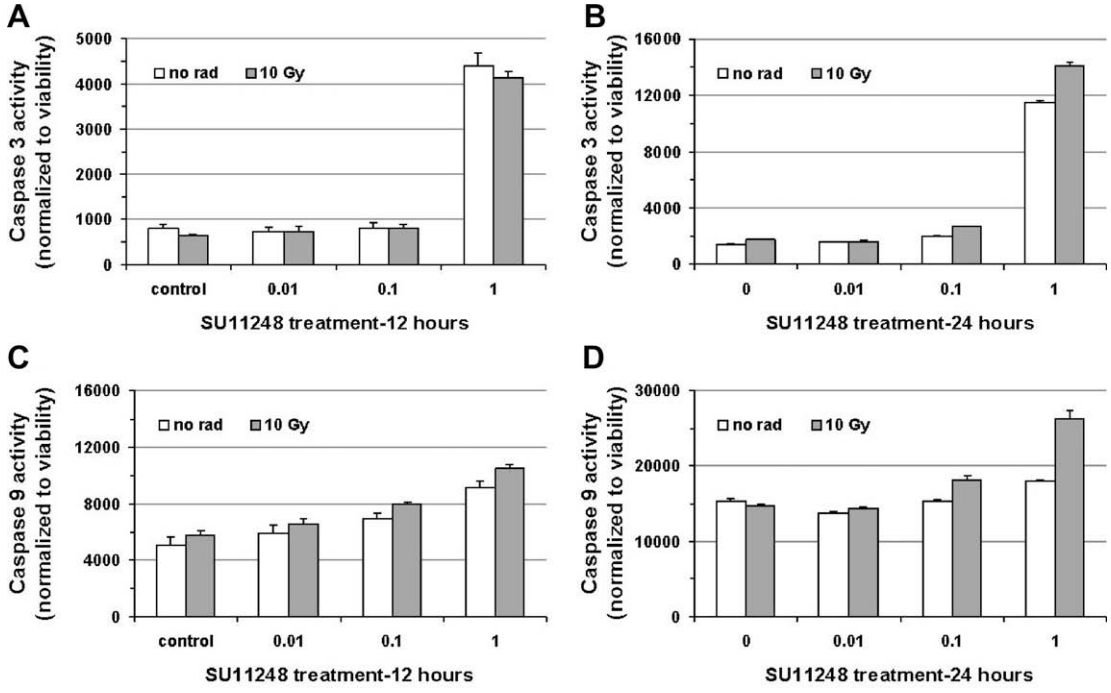

Fig. 2 – Effect of SU11248 and 10 Gy of radiation on the activity of caspase-3 (A and B) and caspase-9 (C and D) in 4T1 cells. Values represent means ± SE ($n = 3$, $P < 0.05$).

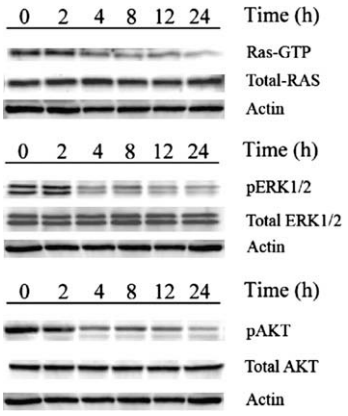

Fig. 3 – SU11248 suppresses cell signalling within Ras, Erk1/2 and AKT molecular pathway in 4T1 cells. Western blots were performed with antibodies to Ras-GTP (A), phospho-Erk1/2 (B) and phospho-Akt (C). Actin as well as anti-Ras, -Erk1/2 and -AKT antibodies were used as protein quantitative controls for each of the collected samples.

3.5. *MVD in bone tumour*

The analysis of MVD in tumour-bearing animals showed 245.7 ± 7.67 microvessels per mm^2 (Fig. 5B). Local irradiation treatment did not decrease the number of microvessels in murine 4T1 breast cancer tumours as compared to the control animals. However, SU11248 alone or in combination with radiation reduced MVD in viable tumour to 191.8 ± 6.46 and 153.7 ± 5.83 microvessels per mm^2, respectively ($P < 0.05$ versus tumour-bearing mice). This suggests that the antiangiogenic activity of SU11248 may be partially responsible for the radiosensitisation of 4T1 tumour cells.

3.6. *Tumour-induced bone pain*

Ongoing pain was evaluated using the measurements of spontaneous guarding and flinching over a 2-min time period on day 16 after tumour injection. All treatments were administered on day 7. Tumour-bearing controls spent a greater time in guarding, and flinched more often as compared to the saline-injected controls (Fig. 6A and B). Combination treatment

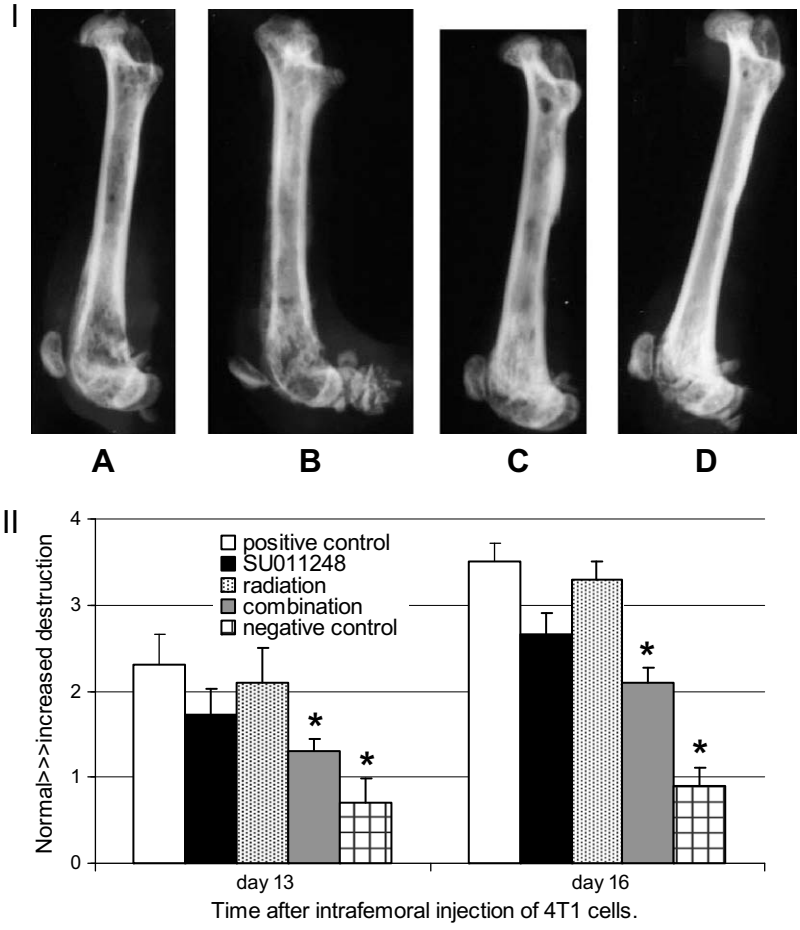

Fig. 4 – SU11248 plus radiation reduces femoral destruction following the injection of 4T1 cells. (I) *Femur radiographs:* Treatments were started on day 7 after the intrafemoral injection of 4T1 cells with saline as a positive control (A), irradiation with 15 Gy in a single fraction (B), SU011248 with 40 mg/kg (C) and the combination of SU011248 and irradiation (D). Radiographs were taken on day 16 and are representative of 10 mice. (II) *Bone destruction scores:* Assessment of bone destruction in femur radiographs was performed on days 13 and 16 using a grading system of bone lysis with numeric values ranging from 0 to 4. Groups assignments were blinded, *$P < 0.05$ versus control.

alleviated spontaneous guarding compared to the controls (Fig. 6A, $P < 0.05$). The mean number of flinches was highest in the untreated control animals. On day 16, flinching was significantly lower in animals treated with combination versus either treatment alone or untreated controls (Fig. 6B, $P < 0.05$).

Ambulatory pain was assessed using limb use and rotarod tests. Tumour-bearing animals showed increased movement-evoked pain during limb use and forced ambulation (rotarod test) as compared to the saline-injected controls (Fig. 6C and D). Combination treated animals had significantly improved limb use on day 16 (Fig. 6C, $P < 0.05$ versus untreated controls). Moreover, combination treatment resulted in less guarding during forced movement on the rotarod wheel as compared to the tumour-bearing animals (Fig. 6D), but there was no significant difference compared to the radiation-only or SU011248-only groups.

3.7. *Prodynorphin and GFAP immunoreactivity in L4–L5 spinal cord sections*

To examine the effect of combination treatment on neurochemical changes in L4–L5 spinal cord sections, we quantified the immunoreactivity of prodynorphin and GFAP. Animals injected with 4T1 breast cancer cells into the left femora demonstrated the increased expression of prodynorphin in the ipsilateral L4–L5 spinal cord sections as compared to the contralateral sections from the same animal. Combination treatment significantly reduced the expression of prodynorphin in ipsilateral dorsal horn neurons located in laminae II–VI compared to ipsilateral sections in tumour-bearing controls (Fig. 6E and F). In addition, combination treatment significantly decreased the expression of prodynorphin in ipsilateral dorsal horn neurons versus the radiation-only group ($P < 0.031$) and SU11248-only group ($P < 0.038$). In addition, a massive astrogliosis was present throughout the ipsilateral spinal cord section, which received primary afferent innervation from tumour-bearing femora. Combination treatment decreased GFAP immunoreactivity (astrogliosis) in ipsilateral sections on day 16 compared to the untreated animals ($P < 0.001$; Fig. 6E and G). Also, the combination treatment group had a significantly lower expression of GFAP versus radiation alone ($P < 0.016$). There was no statistical difference in GFAP expression between combination and SU11248 alone.

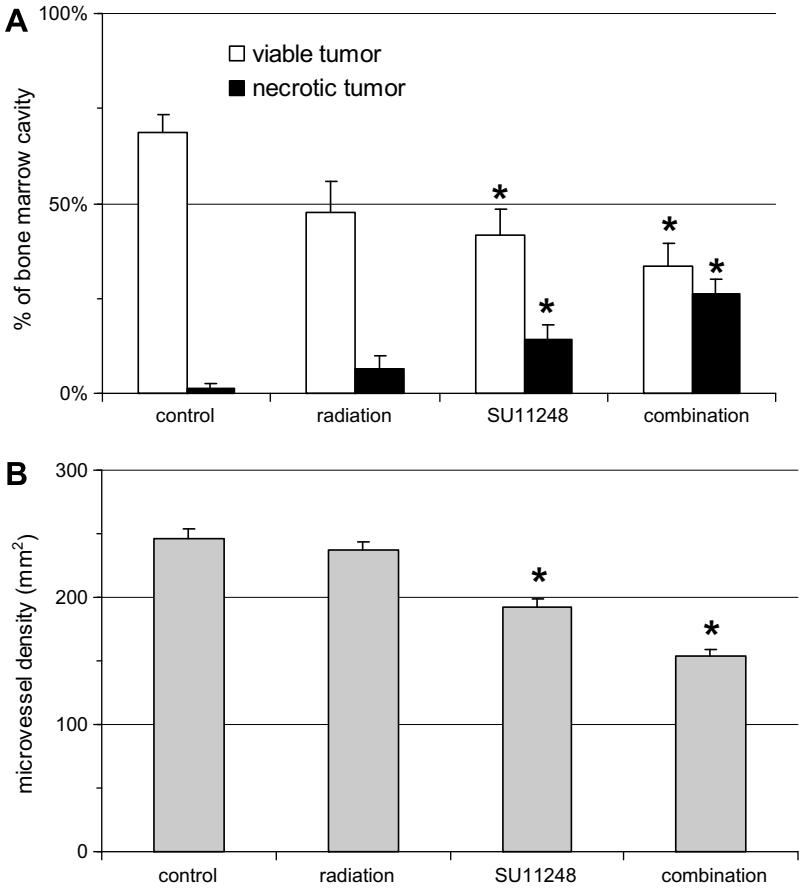

Fig. 5 – (A) SU11248 plus local radiation decreases viable tumour area and increases tumour necrosis. Tumour necrosis was measured in femoral sections (bone marrow cavity) as the percent of total tumour cells showing the signs of cell death (eosinophilic cells that did not display prominent nuclei). Viable tumour area was expressed as a percent of intramedullary space occupied by tumour cells displaying nuclei. (B) SU11248 plus local radiation reduces MVD in bone tumour. Immunohistochemical data from 4T1 breast tumour tissue stained for CD31 were quantified. *P-values < 0.05 versus untreated animals. Values represent means ± SEM. Untreated, tumour-bearing mice were used as a control.

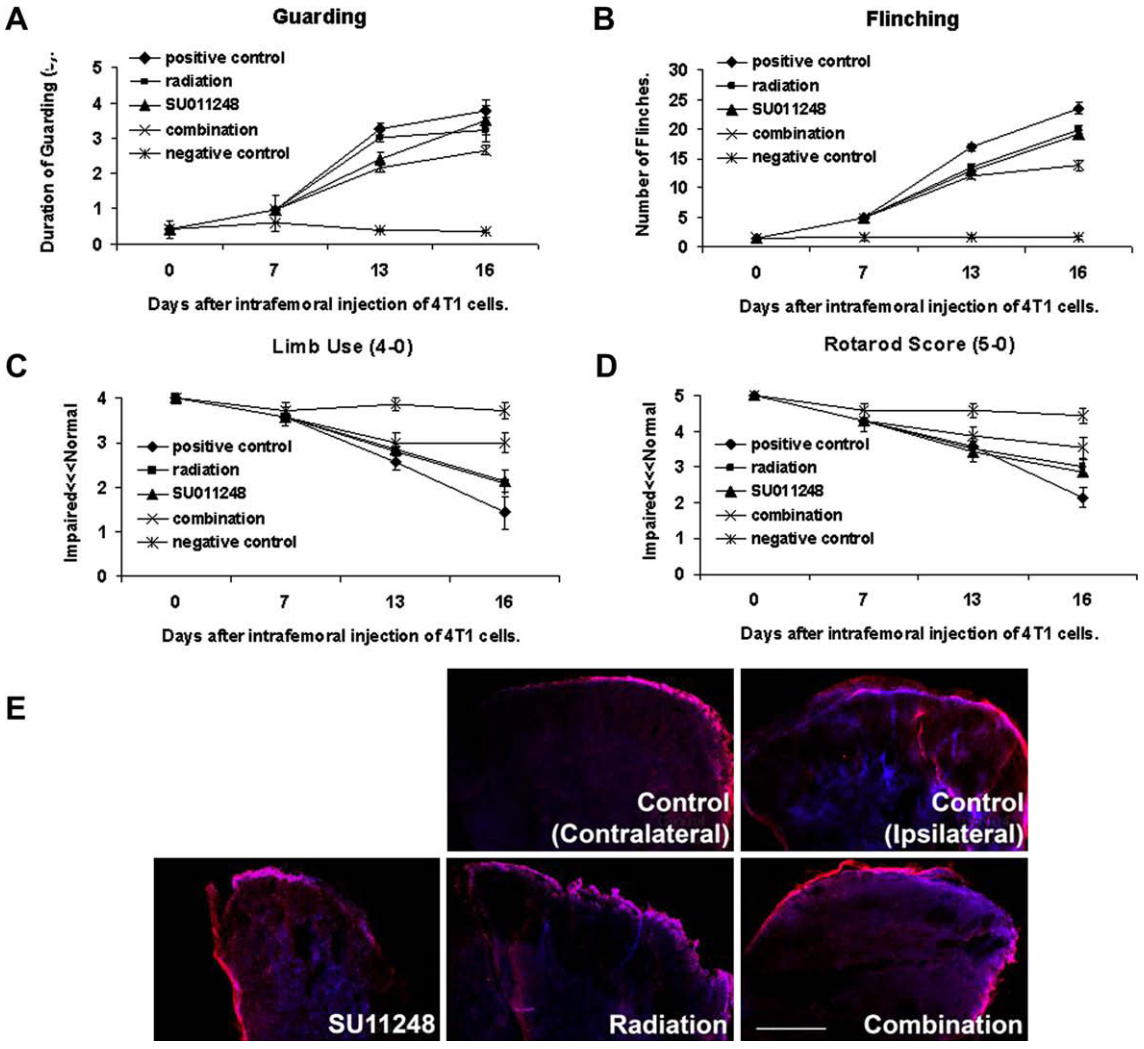

Fig. 6 – SU11248 plus local radiation reduces cancer-induced bone pain. Spontaneous and movement-evoked measurements of pain were measured for mice with 4T1 tumours in the left femora. (A and B) Duration of spontaneous guarding and number of spontaneous flinches over a 2-min observation period was used as a measure of ongoing pain on days 7, 13 and 16. (C and D) Movement-evoked pain was assessed using spontaneous limb use and guarding during forced ambulation on a Rotarod. Limb use scores were based on a 0–4 scoring system, with 4 defined as normal limb use, 3 pronounced limping, 2 limping and guarding, 1 partial non-use and 0 complete loss of limb use. Rotarod scores were defined as follows: the animal held the affected limb completely aloft; a score of 5 indicated normal limb use, 4 presence of minimal guarding, 3 pronounced guarding, 2 pronounced guarding accompanied by limping, 1 partial non-use and 0 complete loss of limb use. Values represent means ± SEM. (E) Immunohistochemical staining of spinal cords. Confocal images show the distribution of prodynorphin (red) and GFAP (blue) in laminae I–II and III–VI of the dorsal horn in coronal sections of the L4–L5 spinal segment on day 16 following injection of 4T1 cells into the left femora. Cord sections were stained with polyclonal antibodies to prodynorphin and GFAP. Images are representative of montages of three subsequent sections for each animal in each animal group. Scale bar = 200 μm. (F and G) Quantification of prodynorphin (B-I) and GFAP (B-II) immunoreactivity in L4–L5 spinal sections obtained from each treatment group, $n = 10$ ($^{*}P < 0.05$).

4. Discussion

The multiple fractions of radiation required in patients with bone metastases are often insufficient to provide complete pain relief and prevent increased risk of pathologic fractures in long bones.[12–14] In this study, we demonstrate that antiangiogenic therapy with SU11248 has the potential to enhance the effectiveness of single-dose or short-course radiation treatment in these patients. We show that tumour growth, bone osteolysis and cancer-induced bone pain all improved following combination treatment in an orthotopic *in vivo* model of metastatic breast cancer in bone. Compared to either SU11248 or local irradiation alone, their combination decreased MVD in viable tumour, reduced the area of viable

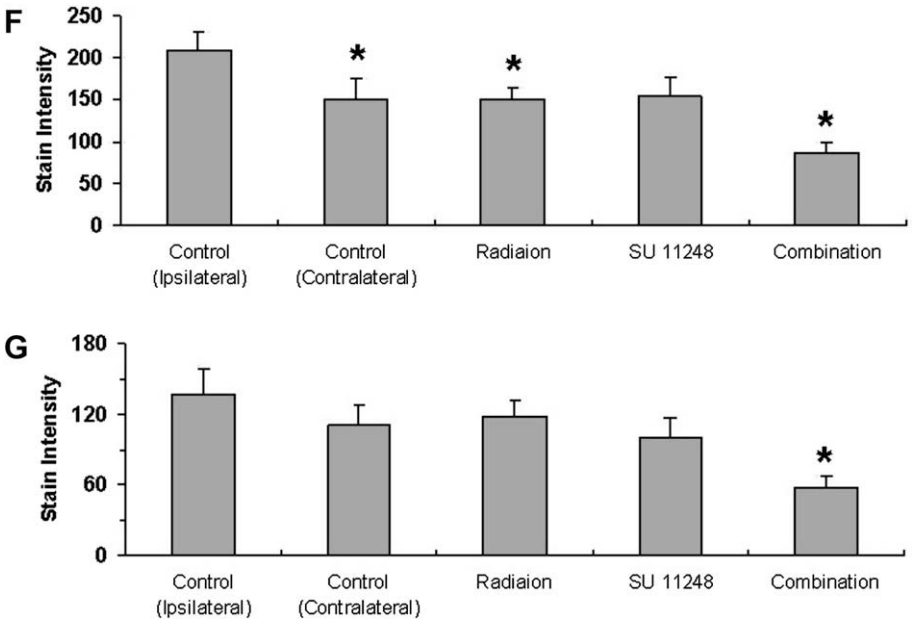

Fig. 6 (*continued*)

tumour and increased tumour necrosis in the bone marrow cavity. This *in vivo* anti-tumour activity is consistent with our *in vitro* data showing the increased levels of caspase-3 and -9 in cultured 4T1 breast cancer cells after 24 h exposure to SU11248 and radiation, suggesting that the caspase-induced apoptosis is partly responsible for the radiosensitising effects of SU11248.

Recent reports have demonstrated that the activation of the Ras signalling pathway increases the survival of tumour cells exposed to radiation.[37,38] We observed the decreased phosphorylation of Ras in a time-dependent manner after treatment with SU11248. SU11248 also inhibited the phosphorylation of two downstream substrates of phosphorylated Ras, ERK1/2 and AKT, at 24 h post-SU11248 treatment. Our results suggest that the Ras signalling pathway might be targeted by SU11248 to enhance the radiosensitivity of metastatic bone tumours.

Pain is a significant morbidity associated with the breast cancer metastasising to bone. In this study, combination treatment resulted in improved pain relief, and reduced bone destruction and neuronal dysregulation. The evaluation of bone destruction demonstrated significantly reduced bone scores in combination treatment versus either treatment alone. Behavioural analysis showed that SU11248 in combination with local irradiation significantly improved ongoing as well as ambulatory pain. This functional improvement might be a result of reduction in tumour size and the number of activated osteoclasts. We observed that radiation alone did reduce pain behaviours in the first days after treatment, but this effect disappeared possibly because of tumour regrowth. It has been reported that radiation-induced cell death or cell arrest primarily occurs within 24 h in most cell types.[39,40] In contrast, radiation in combination with SU11248 was associated with a prolonged period of decreased ongoing and ambulatory pain behaviours, most probably because of the increased cytotoxicity of combination treatment.

Recent reports have also shown that primary afferent neurons innervating the periostium may be sensitised by low pH produced by osteoclasts and cancer cells.[41,42] Moreover, many different cancer types produce growth factors and cytokines that can directly stimulate primary afferent neurons.[43,44] In this study, spinal cord segments receiving primary innervation from tumour-bearing femora demonstrated significant astrocyte hypertrophy, as indicated by GFAP immunoreactivity. This finding is consistent with the previous reports.[45,46] Astrocytes that have undergone hypertrophy produce and release cytokines and growth factors.[47,48] Consistent with our findings, increased expression of the pro-hyperalgesic peptide prodynorphin in neurons located in the deep spinal laminae has been associated with bone cancer pain.[46] In this study, prodynorphin and GFAP expression in L4–L5 spinal cord sections was significantly lower in mice treated with SU11248 and radiation, possibly because of the increased cytotoxicity to tumour cells of this combination treatment. Antiangiogenic therapy has also been shown to stabilise blood vessels,[49] which may have resulted in improved blood flow and subsequently decreased pain stimulus due to the less acidic environment in the tumour/bone zone.

Jain[50] has previously proposed that antiangiogenic therapy could normalise tumour blood vessels and thereby transiently improve blood flow and oxygen supply to the existing tumour tissue. This improvement in the intratumoural blood supply, however, would not provide sufficient oxygen to peripheral tumour tissue and would not result in an increased tumour growth. We posit that SU11248 improves intratumoural blood flow and helps to remove intratumoural metabolites that contribute to the hypoxic environment. This in turn increases the radiosensitivity of intratumoural tumour tissue but at the same time prevents the development of new blood vessels that are necessary for continued tumour growth.

In conclusion, we demonstrate in this study that the addition of an RTK inhibitor to radiation significantly reduces

tumour growth, bone destruction and cancer-related pain. Further studies of this combined modality treatment are therefore warranted.

Conflict of interest statement

Honoraria: Arkadiusz Z. Dudek, Pfizer Speaker's Bureau.

Acknowledgements

The authors would like to thank Michael Franklin for editorial support. We would like to acknowledge the use of confocal microscope made available through an NCRR Shared Instrumentation Grant (No. 1 S10 RR16851).

REFERENCES

1. Coleman RE, Rubens RD. The clinical course of bone metastases from breast cancer. *Br J Cancer* 1987;**55**(1):61–6.
2. Perez EA. Current management of metastatic breast cancer. *Semin Oncol* 1999;**26**(4 Suppl. 12):1–10.
3. Domchek SM, Younger J, Finkelstein DM, Seiden MV. Predictors of skeletal complications in patients with metastatic breast carcinoma. *Cancer* 2000;**89**(2):363–8.
4. Ripamonti C, Dickerson ED. Strategies for the treatment of cancer pain in the new millennium. *Drugs* 2001;**61**(7):955–77.
5. Narazaki DK, de Alverga Neto CC, Baptista AM, Caiero MT, de Camargo OP. Prognostic factors in pathologic fractures secondary to metastatic tumors. *Clinics* 2006;**61**(4):313–20.
6. Wu JS, Wong RK, Lloyd NS, Johnston M, Bezjak A, Whelan T. Radiotherapy fractionation for the palliation of uncomplicated painful bone metastases – an evidence-based practice guideline. *BMC Cancer* 2004;**4**:71.
7. Rodriguez MJ, Contreras D, Galvez R, et al. Double-blind evaluation of short-term analgesic efficacy of orally administered dexketoprofen trometamol and ketorolac in bone cancer pain. *Pain* 2003;**104**(1–2):103–10.
8. Mystakidou K, Katsouda E, Kouloulias V, Kouvaris J, Tsiatas M, Vlahos L. Comparison of transdermal fentanyl with codeine/paracetamol, in combination with radiotherapy, for the management of metastatic bone pain. *J Opioid Manag* 2005;**1**(4):204–10.
9. Blum RH, Novetsky D, Shasha D, Fleishman S. The multidisciplinary approach to bone metastases. *Oncology (Williston Park)* 2003;**17**(6):845–57 (discussion 62-3, 67).
10. King T, Gardell LR, Wang R, et al. Role of NK-1 neurotransmission in opioid-induced hyperalgesia. *Pain* 2005;**116**(3):276–88.
11. Gupta K, Kshirsagar S, Chang L, et al. Morphine stimulates angiogenesis by activating proangiogenic and survival-promoting signaling and promotes breast tumor growth. *Cancer Res* 2002;**62**(15):4491–8.
12. Qasim MM. Single dose palliative irradiation for bony metastasis. *Strahlentherapie* 1977;**153**(8):531–2.
13. Tong D, Gillick L, Hendrickson FR. The palliation of symptomatic osseous metastases: final results of the study by the Radiation Therapy Oncology Group. *Cancer* 1982;**50**(5):893–9.
14. Blitzer PH. Reanalysis of the RTOG study of the palliation of symptomatic osseous metastasis. *Cancer* 1985;**55**(7):1468–72.
15. Mendel DB, Laird AD, Xin X, et al. *In vivo* antitumor activity of SU11248, a novel tyrosine kinase inhibitor targeting vascular endothelial growth factor and platelet-derived growth factor receptors: determination of a pharmacokinetic/pharmacodynamic relationship. *Clin Cancer Res* 2003;**9**(1):327–37.
16. O'Farrell AM, Abrams TJ, Yuen HA, et al. SU11248 is a novel FLT3 tyrosine kinase inhibitor with potent activity *in vitro* and *in vivo*. *Blood* 2003;**101**(9):3597–605.
17. Ostman A, Heldin CH. PDGF receptors as targets in tumor treatment. *Adv Cancer Res* 2007;**97**:247–74.
18. Oh HK, Ha JM, O E, Lee BH, Lee SK, Shim BS, et al. Tumor angiogenesis promoted by *ex vivo* differentiated endothelial progenitor cells is effectively inhibited by an angiogenesis inhibitor, TK1-2. *Cancer Res* 2007;**67**(10):4851–9.
19. Gorski DH, Beckett MA, Jaskowiak NT, et al. Blockage of the vascular endothelial growth factor stress response increases the antitumor effects of ionizing radiation. *Cancer Res* 1999;**59**(14):3374–8.
20. Kozin SV, Boucher Y, Hicklin DJ, Bohlen P, Jain RK, Suit HD. Vascular endothelial growth factor receptor-2-blocking antibody potentiates radiation-induced long-term control of human tumor xenografts. *Cancer Res* 2001;**61**(1):39–44.
21. Schueneman AJ, Himmelfarb E, Geng L, et al. SU11248 maintenance therapy prevents tumor regrowth after fractionated irradiation of murine tumor models. *Cancer Res* 2003;**63**(14):4009–16.
22. Griffin RJ, Williams BW, Wild R, Cherrington JM, Park H, Song CW. Simultaneous inhibition of the receptor kinase activity of vascular endothelial, fibroblast, and platelet-derived growth factors suppresses tumor growth and enhances tumor radiation response. *Cancer Res* 2002;**62**(6):1702–6.
23. Zwolak P, Dudek AZ, Bodempudi VD, et al. Local irradiation in combination with bevacizumab enhances radiation control of bone destruction and cancer-induced pain in a model of bone metastases. *Int J Cancer* 2008;**122**(3):681–8.
24. Dudek AZ, Zwolak P, Jasinski P, et al. Protein kinase C-beta inhibitor enzastaurin (LY317615. *HCI) enhances radiation control of murine breast cancer in an orthotopic model of bone metastasis. Invest New Drugs* 2008;**26**(1):13–24.
25. Goblirsch M, Zwolak P, Ramnaraine ML, et al. Novel cytosine deaminase fusion gene enhances the effect of radiation on breast cancer in bone by reducing tumor burden, osteolysis, and skeletal fracture. *Clin Cancer Res* 2006;**12**(10):3168–76.
26. Goblirsch MJ, Zwolak P, Clohisy DR. Advances in understanding bone cancer pain. *J Cell Biochem* 2005;**96**(4):682–8.
27. Goblirsch M, Mathews W, Lynch C, et al. Radiation treatment decreases bone cancer pain, osteolysis and tumor size. *Radiat Res* 2004;**161**(2):228–34.
28. Murray LJ, Abrams TJ, Long KR, et al. SU11248 inhibits tumor growth and CSF-1R-dependent osteolysis in an experimental breast cancer bone metastasis model. *Clin Exp Metastasis* 2003;**20**(8):757–66.
29. Weber KL, Doucet M, Price JE, Baker C, Kim SJ, Fidler IJ. Blockade of epidermal growth factor receptor signaling leads to inhibition of renal cell carcinoma growth in the bone of nude mice. *Cancer Res* 2003;**63**(11):2940–7.
30. Honore P, Luger NM, Sabino MA, et al. Osteoprotegerin blocks bone cancer-induced skeletal destruction, skeletal pain and pain-related neurochemical reorganization of the spinal cord. *Nat Med* 2000;**6**(5):521–8.
31. Lees RL, Heersche JN. Macrophage colony stimulating factor increases bone resorption in dispersed osteoclast cultures by increasing osteoclast size. *J Bone Miner Res* 1999;**14**(6):937–45.
32. Yoneda J, Kuniyasu H, Crispens MA, Price JE, Bucana CD, Fidler IJ. Expression of angiogenesis-related genes and progression of human ovarian carcinomas in nude mice. *J Natl Cancer Inst* 1998;**90**(6):447–54.
33. Wacnik PW, Baker CM, Herron MJ, et al. Tumor-induced mechanical hyperalgesia involves CGRP receptors and altered

innervation and vascularization of DsRed2 fluorescent hindpaw tumors. *Pain* 2005;**115**(1–2):95–106.
34. Pan J, Yeger H, Cutz E. Innervation of pulmonary neuroendocrine cells and neuroepithelial bodies in developing rabbit lung. *J Histochem Cytochem* 2004;**52**(3):379–89.
35. Lynch JL, Gallus NJ, Ericson ME, Beitz AJ. Analysis of nociception, sex and peripheral nerve innervation in the TMEV animal model of multiple sclerosis. *Pain* 2008;**136**(3):293–304.
36. Mihm MJ, Schanbacher BL, Wallace BL, Wallace LJ, Uretsky NJ, Bauer JA. Free 3-nitrotyrosine causes striatal neurodegeneration *in vivo*. *J Neurosci* 2001;**21**(11):RC149.
37. Kim IA, Bae SS, Fernandes A, et al. Selective inhibition of Ras, phosphoinositide 3 kinase, and Akt isoforms increases the radiosensitivity of human carcinoma cell lines. *Cancer Res* 2005;**65**(17):7902–10.
38. Kim IA, Fernandes AT, Gupta AK, McKenna WG, Bernhard EJ. The influence of Ras pathway signaling on tumor radiosensitivity. *Cancer Metastasis Rev* 2004;**23**(3–4):227–36.
39. Dainiak N. Practical and theoretical issues in 1993 concerning radiation effects on the growth of normal and neoplastic hematopoietic cells. *Stem Cells* 1997;**15**(Suppl. 2):75–85.
40. Held KD. Radiation-induced apoptosis and its relationship to loss of clonogenic survival. *Apoptosis* 1997;**2**(3):265–82.
41. Gillies RJ, Liu Z, Bhujwalla Z. 31P-MRS measurements of extracellular pH of tumors using 3-aminopropylphosphonate. *Am J Physiol* 1994;**267**(1 Pt 1):C195–203.
42. Griffiths JR. Are cancer cells acidic? *Br J Cancer* 1991;**64**(3):425–7.
43. Woolf CJ, Allchorne A, Safieh-Garabedian B, Poole S. Cytokines, nerve growth factor and inflammatory hyperalgesia: the contribution of tumour necrosis factor alpha. *Br J Pharmacol* 1997;**121**(3):417–24.
44. Suzuki K, Yamada S. Ascites sarcoma 180, a tumor associated with hypercalcemia, secretes potent bone-resorbing factors including transforming growth factor alpha, interleukin-1 alpha and interleukin-6. *Bone Miner* 1994;**27**(3):219–33.
45. Schwei MJ, Honore P, Rogers SD, et al. Neurochemical and cellular reorganization of the spinal cord in a murine model of bone cancer pain. *J Neurosci* 1999;**19**(24):10886–97.
46. Honore P, Rogers SD, Schwei MJ, et al. Murine models of inflammatory, neuropathic and cancer pain each generates a unique set of neurochemical changes in the spinal cord and sensory neurons. *Neuroscience* 2000;**98**(3):585–98.
47. Bruno V, Battaglia G, Casabona G, Copani A, Caciagli F, Nicoletti F. Neuroprotection by glial metabotropic glutamate receptors is mediated by transforming growth factor-beta. *J Neurosci* 1998;**18**(23):9594–600.
48. Hori O, Matsumoto M, Kuwabara K, et al. Exposure of astrocytes to hypoxia/reoxygenation enhances expression of glucose-regulated protein 78 facilitating astrocyte release of the neuroprotective cytokine interleukin 6. *J Neurochem* 1996;**66**(3):973–9.
49. Duda DG, Jain RK, Willett CG. Antiangiogenics: the potential role of integrating this novel treatment modality with chemoradiation for solid cancers. *J Clin Oncol* 2007;**25**(26):4033–42.
50. Jain RK. Normalization of tumor vasculature: an emerging concept in antiangiogenic therapy. *Science* 2005;**307**(5706):58–62.